

The Shrinking "Fermi-Arc" in Cuprates

C. M. Varma and Lijun Zhu

Department of Physics, University of California, Riverside, California 92521

The angle-resolved photoemission spectroscopy (ARPES) studies on cuprates in the pseudogap region reveal an extraordinary topological transition in which the ground state changes from one with a usual Fermi surface to one with four fermi-points. We show that the experimental results are quantitatively given without any free parameters by a theory and discuss the implications of the results.

PACS numbers: 74.25.Jb, 74.20.-z, 74.72.-h

Recently the single-particle spectral function $A(\mathbf{k}, \omega)$ obtained by ARPES on six different underdoped BSCCO cuprates with T_c ranging from 20K to 89K have been systematically analyzed [1]. The principal conclusion is that the angular region in $\hat{\mathbf{k}}$ where $A(\mathbf{k}, \omega)$ has a maxima at the chemical potential μ for any $|\mathbf{k}|$, is a universal function $\Phi(T/T_g(x))$. T is the temperature and $T_g(x)$ is the pseudogap temperature at x , the deviation of the density of holes from half-filling. $T_g(x)$ is, within the uncertainties of its determination, the same as that obtained from the resistivity or the thermodynamic measurements such as the magnetic susceptibility and the specific heat which also scale as functions of $(T/T_g(x))$ [2]. At $T \geq T_g(x)$, $\Phi = 2\pi$, i.e. the angular region encloses an area, while for $T \rightarrow 0$, $\Phi \rightarrow 0$, i.e. the region shrinks to 4 points.

Recall that in a Fermi-liquid [3] (or a marginal Fermi-liquid [4]), $A(\mathbf{k}, \omega)$ is maximum at $\omega = \mu$ for $\mathbf{k} = \mathbf{k}_F$, thus defining the fermi-surface. The concept of a fermi-surface, properly defined as the non-analytic surface which separates the area of occupied states from the unoccupied states, is strictly meaningful only at $T \rightarrow 0$. This is merely a technicality in the usual metallic state. But for underdoped cuprates, the proper definition of a fermi-surface is essential. The experimental results show that for $x > x_c$, such that $T_g(x_c) = 0$, the extrapolated $T = 0$ non-superconducting groundstate has a fermi-surface. For $x < x_c$, the groundstate does not have a fermi-surface; it only has four fermi-points.

These experimental results are in accord with a theory of the pseudogap state [5, 6] which specifically predicted that the ground state of the underdoped state has only four fermi-points and that the evolution of the single-particle spectra is a universal function of $(T/T_g(x))$. In this note, we show that the function $\Phi(T/T_g(x))$, as defined above and used by the experimentalists [1] to organize the central features of the data, is quantitatively given by the theory; we also make a few remarks about its significance and how it affects the theories of the cuprates.

It has become the custom to call the angular region $\Phi(T/T_g)$, a *fermi-arc*. This is only harmless if the empirical procedure used to derive $\Phi(T/T_g)$ from the experiments is kept in mind.

The change of the connectivity of the fermi-surface without change of symmetry was described by Lifshitz

[7, 8] many years ago. Quite clearly, the shrinking of the fermi-surface to four points, while retaining all the symmetries is an extreme case of such a topological transition. However the topological transition may well accompany some symmetry change [8]. This happens, for example at the superfluid transition to the A phase in liquid ^3He , where the fermi-surface also shrinks to points.

In a theory of the cuprates [5, 6], this topological change accompanies a transition to a state with orbital current loops (which breaks time-reversal and certain reflections but preserves the translational symmetry of the crystal). Dichroism in ARPES was predicted [9] in such a state and has been observed [10, 11]. More recently polarized neutron diffraction experiments have directly observed [12] magnetic scattering at Bragg spots for $T \lesssim T_g(x)$, consistent with the proposed pattern of loops.

A fermi-surface was shown to be unstable in the presence of such a symmetry change [5, 6]. The single-particle spectrum at $T \rightarrow 0$ in the stable state in the absence of impurity scattering has eigenvalues given by

$$E_{\mathbf{k}}^{>,<} = \epsilon_{\mathbf{k}} \pm D(\mathbf{k}), \text{ for } E_{\mathbf{k}} > (\text{or } <) \mu, \quad (1)$$

where $D(\mathbf{k}) \approx D_0(1 - T/T_g)^{1/2} \cos^2(2\phi)/[1 + (\epsilon_{\mathbf{k}}/\epsilon_c)^2]$ is the gap function, which is anisotropic and temperature-dependent. ϕ is the angle of $\hat{\mathbf{k}}$ and $\epsilon_{\mathbf{k}}$ is the "band-structure" energy, which is taken from a tight-binding model with nearest-neighbor hopping t and next-nearest-neighbor t' adopted to fit the fermi-surface found by ARPES for $x \leq x_c$ to be

$$\epsilon_{\mathbf{k}} = -2t[\cos k_x + \cos k_y] - 4t' \cos k_x \cos k_y, \quad (2)$$

where $t'/t = -0.35$. ϵ_c is a cut-off of order D_0 . The simple theory [6] gives $D_0 \approx \sqrt{6}T_g$.

The single-particle spectrum is given by the spectral function

$$A^{>,<}(\mathbf{k}, \omega) = -\frac{1}{\pi} \frac{\text{Im}\Sigma(\mathbf{k}, \omega)}{[\omega - E_{\mathbf{k}}^{>,<} - \text{Re}\Sigma(\mathbf{k}, \omega)]^2 + [\text{Im}\Sigma(\mathbf{k}, \omega)]^2}, \quad (3)$$

where $\Sigma(\mathbf{k}, \omega)$ is the self-energy, which is the sum of the contribution due to electron-electron scattering. We present here results in the pure limit as well as including small angle impurity scattering. If $-\text{Im}\Sigma \gtrsim D(\mathbf{k}_F)$, the

spectrum $A^>(\mathbf{k}, \omega)$ has finite weight in the $\omega < \mu$ region measured by ARPES. So, the total spectrum measured by ARPES (at $\omega \leq \mu$) is

$$A(\mathbf{k}, \omega \leq \mu) = A^<(\mathbf{k}, \omega) + A^>(\mathbf{k}, \omega). \quad (4)$$

$\Sigma(\mathbf{k}, \omega)$ away from the zeroes of $D(\hat{\mathbf{k}})$, i.e. away from the *nodal* region is calculated in the pure limit to be

$$-\text{Im}\Sigma_{in}(\mathbf{k}, \omega, T) = \text{sech} \left(\frac{D(\mathbf{k})}{\sqrt{\omega^2 + \pi^2 T^2}} \right) \tau_M^{-1}(\omega, T) \quad (5)$$

where τ_M^{-1} is the marginal fermi-liquid relaxation rate:

$$\tau_M^{-1} = \lambda \sqrt{\omega^2 + \pi^2 T^2}. \quad (6)$$

Near the zeroes of $D(\hat{\mathbf{k}})$, the self-energy for $\omega \ll D_0(\mathbf{k})$ is

$$-\text{Im}\Sigma_{in}(\mathbf{k}, \omega, T) = \lambda \frac{\omega^2}{D_0}, \quad (7)$$

while for $\omega \gg D(\mathbf{k})$, it reverts to the MFL form. An interpolation form, such as in Eq.(5) may be used to connect the two limits. In our calculations below, we have used Eq. (7) for a region extending to $\pi/20$ about the nodal regions and Eq.(5) elsewhere. Similar results are obtained for factors of 2 variations about this partitioning.

Results and Comparison with Experiments. The spectral function is calculated using Eqs.(3,4). The parameters used in the evaluation are $D_0/T_g = 2.5$ and λ is fixed by the value determined by the MFL fits to the spectral function for $x \geq x_c$ to be ≈ 0.5 . Earlier, the specific heat and the magnetic susceptibility in the underdoped cuprates was fit [6] to experiments with $D_0/T_g \approx 2.5$. Thus there are no free parameters left to fit.

In Fig. 1, the calculated spectral function is plotted at the anti-nodal point for various T/T_g and for various angles at $T/T_g = 0.5$. The inset shows the definition of various quantities used to represent the experiments in Ref.[1]. These definitions are used to compare with experiments in Figs. 2 and 3. $\Delta(\phi)$ is defined as the energy at which the spectral function peaks below the chemical potential at the angle ϕ , while $I(0)$ and $I(\Delta)$ are the intensities at the chemical potential and at Δ , respectively. Either $\Delta = 0$ or $1 - I(0)/I(\Delta) = 0$ implies that $A(\mathbf{k}_F, \omega)$ reaches its maxima at the chemical potential.

The experimental results and the calculated values of $\Delta(\phi)/\Delta(0)$ and of $I(\Delta)/I(0)$ are shown in Fig. 2. The central aspect of the experimental results deduced from the experiments, is shown in Fig. 3 together with the results of calculations. Fig. 3 shows that the "fermi-arc", Φ for a whole range of underdoped cuprates at various dopings x is a universal function of $T/T_g(x)$ and that at $T \rightarrow 0, \Phi \rightarrow 0$. The theoretical curve is calculated with $D_0/T_g = 2.5$ and $\lambda = 0.5$. The theory in the pure limit is in quantitative accord with the experimental curve without any free parameters.

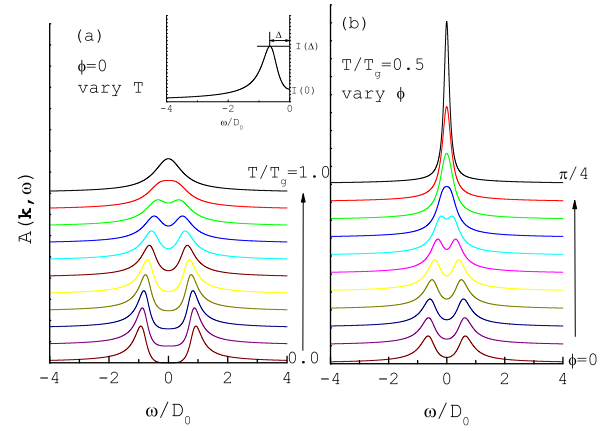


FIG. 1: The spectral functions for (a) fixed angle(antinode) while varying temperatures; (b) fixed temperature ($T/T_g = 0.5$) while varying angles from antinode to node. Here, $D_0 = 2.5T_g$. As shown in inset, we have followed the representation of the data as in experiments to define the position of the peak relative to the chemical potential Δ , the intensity of the spectral function at Δ and the chemical potential as $I(\Delta)$, $I(0)$, respectively.

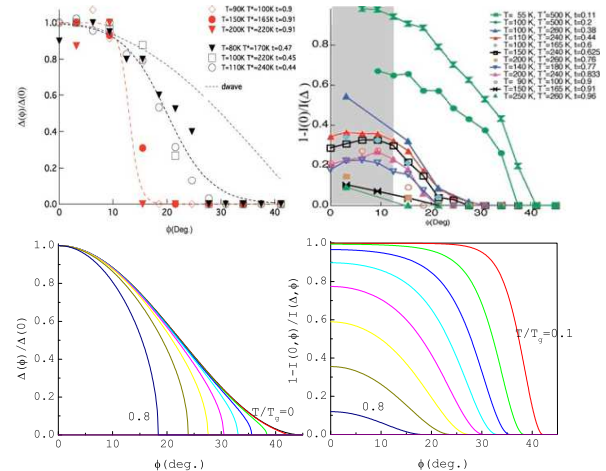


FIG. 2: The gap and the peak intensity as functions of the angle. The experimental data are also shown(above). They are employed to determine the fermi arc length.

The agreement actually is a little worse if we include impurity scattering, see Fig. 4. We have calculated the spectral function including the effects of small angle scattering due to impurities in between the Cu-O planes [13, 14]. Due to the anisotropy of the density of states in the pseudogap state, the impurity scattering rate becomes anisotropic as well as frequency dependent. With the impurity scattering estimated from experiments

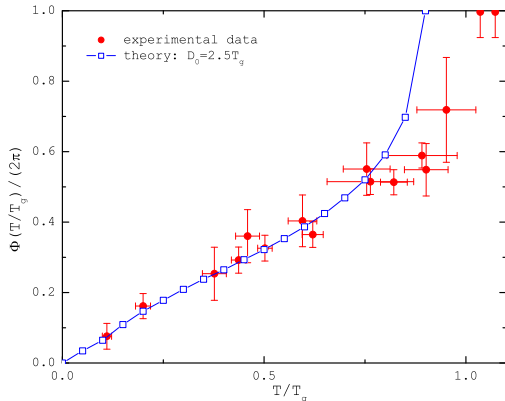


FIG. 3: The fermi-arc length as a function of T/T_g . The experimental data are shown in red dots with error bars. Solid line is the theoretical result without impurity scattering.

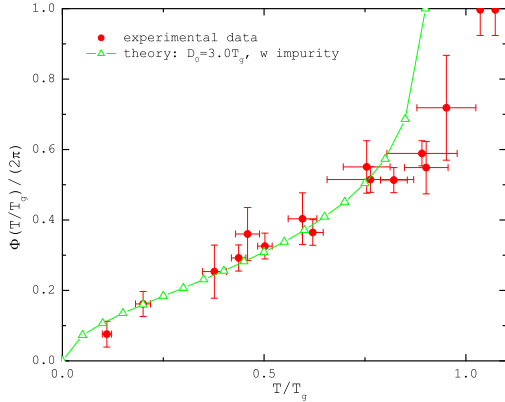


FIG. 4: The fermi-arc length as a function of T/T_g in presence of small-angle impurity scattering. Solid line is the theoretical fit with $D_0 = 3T_g$ and $1/\tau_0 = T_g$, where $1/\tau_0$ is the impurity scattering rate at the nodal point and is independent of the temperature while varies with impurity concentration. Its magnitude can be estimated from the normal state data, such as in Ref. [15].

which gives an elastic scattering rate of about $200K$ at the nodal point above T_g [15], we have to use $D_0/T_g \approx 3$ to get agreement with the experiments. With small angle scattering, only four fermi-points remain at $T \rightarrow 0$ but a weak smooth bump develops for these values at around $D_0/T_g \approx 0.1$, which however continues to give a theoretical curve within the experimental error bars. The impurity scattering of-course varies also from sample to sample. We should also mention that if large angle impurity scattering in the unitary limit were important [16], say due to impurities in the plane, we expect an impurity resonance at the nodal points, so that the fermi-points are smeared out.

General Considerations on Possible Theories. We are not aware of any other theory giving even the qualitative results of the experiments. Since the fermi-surface shrinks to points as temperature decreases without any change in the symmetry, ideas for the pseudogap region based on change of translational symmetry at $T_g(x)$ can be excluded. So also theories which give rise to small pockets of fermi-surface for any other reason. The scaling form $\Phi(T/T_g(x))$ characterizing the spectral function at the chemical potential implies that the phenomena cannot be associated with the superconducting temperature $T_c(x)$. In fact no systematic feature is seen if one plots $\Phi(T/T_c(x))$. In ideas based on regarding the pseudogap phase as a fluctuating phase, either of amplitude or phase of the superconducting order parameter, one expects $\Phi(T)$ to show characteristic features for $T \rightarrow T_c$. Theories which generate anisotropic reduction of the density of states in the underdoped state without generating fermi-points at $T = 0$, such as approximate solutions of the Hubbard model with DMFT or its extensions can also be excluded.

[1] A. Kanigel *et al.*, *Nature Physics* **2**, 447 (2006).
[2] J. W. Loram *et al.*, *J. Phys. Chem. Solids* **62**, 59 (2001); see also, Fig. 8 in Ref. [6].
[3] See, e.g., D. Pines and P. Nozières, *The Theory of Quantum Liquids*, (Benjamin, New York, 1966).
[4] C. M. Varma, P. B. Littlewood, S. Schmitt-Rink, E. Abrahams, and A. E. Ruckenstein, *Phys. Rev. Lett.* **63**, 1996 (1989).
[5] C. M. Varma, *Phys. Rev. Lett.* **83**, 3538 (1999).
[6] C. M. Varma, *Phys. Rev. B* **73**, 155113 (2006).
[7] I. M. Lifshitz, *Zh. Eksp. Teor. Fiz.* **38**, 1569 (1960).
[8] G. E. Volovik, *The Universe in a Helium Droplet*, (Clarendon Press, London, 2003; cond-matt/0601372).
[9] C. M. Varma, *Phys. Rev. B* **61**, R3804 (2000).
[10] A. Kaminski *et al.*, *Nature (London)* **416**, 610 (2002).
[11] M. E. Simon and C. M. Varma *Phys. Rev. Lett.* **89**, 247003 (2002).
[12] B. Fauqué *et al.*, *Phys. Rev. Lett.* **96**, 197001 (2006).
[13] E. Abrahams and C. M. Varma, *Proc. Natl. Acad. Sci. U.S.A.* **97**, 5714 (2000).
[14] E. Abrahams and C. M. Varma, *Phys. Rev. B* **68**, 094502 (2003).

- [15] A. Kaminski *et al.*, Phys. Rev. B **71**, 014517 (2005).
- [16] C. M. Varma and E. Abrahams, Phys. Rev. Lett. **86**, 4652 (2001).